HAL
open science

An effective urban flood model accounting for street-building exchanges

Cécile Choley, Pascal Finaud-Guyot, Pierre-André Garambois, Robert Mose

To cite this version:

Cécile Choley, Pascal Finaud-Guyot, Pierre-André Garambois, Robert Mose. An effective urban flood model accounting for street-building exchanges. SimHydro 21: Models for complex and global water issues – Practices & expectations, Jun 2021, Nice (sophia-antipolis), France. hal-03992011

HAL Id: hal-03992011

https://hal.science/hal-03992011v1

Submitted on 16 Feb 2023

HAL is a multi-disciplinary open access archive for the deposit and dissemination of scientific research documents, whether they are published or not. The documents may come from teaching and research institutions in France or abroad, or from public or private research centers.

L'archive ouverte pluridisciplinaire **HAL**, est destinée au dépôt et à la diffusion de documents scientifiques de niveau recherche, publiés ou non, émanant des établissements d'enseignement et de recherche français ou étrangers, des laboratoires publics ou privés.

AN EFFECTIVE URBAN FLOOD MODEL ACCOUNTING FOR STREET-BUILDING EXCHANGES

Cécile Choley
ENGEES, Icube, Strasbourg, France
cecile.choley@inria.fr

Pascal Finaud-Guyot[1]
Montpellier Univ, HSM, CNRS, IRD, Inria, Montpellier, France
pascal.finaud-guyot@umontpellier.fr

Pierre-André Garambois
Aix-Marseille Univ, INRAE, RECOVER, Aix-en-Provence, France
pierre-andre.garambois@inrae.fr

Robert Mose
IUT Robert Schumann, Icube, Strasbourg, France
mose@unistra.fr

KEY WORDS

Flooding management, Numerical model, Shallow water equations, Street-building exchanges model

ABSTRACT

Floods in cities are a worrying phenomenon as cities concentrate a growing population and activity and are expected to increase in both intensity and frequency in the context of climate change. Flood management provided by public services relies especially on 2D models that do not consider the potential street-building exchanges, considering buildings to be waterproof. A new model is proposed to represent each building as a mass conservation law and an additional source term in the classical 2D shallow water equations. A synthetic test case, with a channel and 200 buildings, shows that the buildings lead to a reduction of both the discharge (30%) and the water depth (18%) peaks in the street and generate a lag time in their time evolution. The interest of the proposed model is highlighted on the modeling of the Richelieu district (Nîmes, France): street-building exchanges impact significantly (up to 0.6 m and 1 m/s) the street hydrodynamics. The water level modifications are generalized in the synthetic case whereas they are more localized in the real-world simulation. Moreover, the model simulates the building water depth allowing for the determination of the maximal level and the submersion duration. These new results pave the way to new information for flood damage analysis and operational management.

1. INTRODUCTION

Floods are among the most frequent and serious natural disasters and are expected to increase in both intensity and frequency due to climate change. According to the World Bank, 29% of the world population is at risk of a 100 years return period flood. By 2050, cities could concentrate 68% of the global population [23] and floods in urban areas are thus of major interest.

Public services are facing an increasing necessity for numerical models to simulate urban floods with accuracy. With the aim of developing and validating innovative numerical approaches, many experimental studies of urban flood processes have been performed over the last 15 years. These works cover urban flooding processes at various scales: from a single crossroad [15] or manhole [2], to a whole street with several inlet and overflow exchange structures [1] and finally to more global urban districts

[1] Corresponding author

[19, 22]. Experiments of urban districts are all based on a flooded street level where the flow invades the streets around the buildings and the building blocks [8]. Nevertheless, some advanced experiments consider additional flow paths such as the invasion of underground volumes (malls, metro, parking...) [10], the river flow over-topping towards an urban area [11], the rain falling directly on the roofs [3] or tsunami waves invading a coastal city [17].

To our best knowledge, few experiments consider water intrusion within buildings: [24] studies the intrusion effect of the hydrodynamic characteristic within the streets, [20] investigates the effect of the building opening on the resultant forces due to flooding. [14] provides lab experiments for a single building along a synthetic channel and a theoretical laws comparison for the discharge entering the building through one opening only similar to a door or a window. None of these works could however measure or even describe the discharge entering the buildings.

Classical practices for urban flood modeling consider the buildings as full or partial obstruction to the flow [18] but neglect in any case the street-building flow exchanges [21] although these exchanges can (i) create a flood retention within blocks and potential reduction of the peak discharge [9], (ii) produce secondary connection between streets through blocks and (iii) explain most part of the damage at the building scale [20, 4]. The lack of models to represent such phenomenon, coherent with an operational application, obliges, for classical approaches on risk management and characterization, to assume that the water level inside the building is the same as in the outside immediate neighboring area.

This paper presents a new modeling approach accounting for the street-building exchanges during a flood event and investigates the potentiality of such model for operational purposes. The model is presented in the first section while the second focuses on model evaluation in both synthetic and real like test cases. The last section proposes concluding remarks and perspectives.

2. MODEL PRESENTATION

The proposed model is based on a 2D representation of the flow within the streets coupled to a reservoir model to represent buildings (inspired form models with lockers); the coupling between the street and the building is represented by different openings. Each building can be connected to several openings pointing to different cells (representing the street). Conversely, a computational cell can be connected to several openings and buildings. The buildings are defined by their area $S_{building}$ and their bottom elevation $z_{b,building}$; the geometry of each opening is rectangular (width: $w_{opening}$). The evolution of the water depth within a building $h_{building}$ is represented with a storage law:

$$\frac{dh_{building}}{dt} = \frac{\sum_{i \in N} Q_i}{S_{building}} \tag{1}$$

where t is the time, Q_i is the discharge through the opening i and N is the set of openings connected to the building.

Using a mass and momentum balance over a control volume within the street, the flows are modeled with the classical 2D shallow water equations:

$$\frac{\partial \boldsymbol{U}}{\partial t} + \frac{\partial \boldsymbol{F}}{\partial x} + \frac{\partial \boldsymbol{G}}{\partial y} = \boldsymbol{S} - \boldsymbol{B} \tag{2a}$$

$$\boldsymbol{U} = \begin{bmatrix} h \\ q \\ r \end{bmatrix};\ \boldsymbol{F} = \begin{bmatrix} q \\ \frac{q^2}{h} + \frac{1}{2}gh^2 \\ \frac{qr}{h} \end{bmatrix};\ \boldsymbol{G} = \begin{bmatrix} r \\ \frac{qr}{h} \\ \frac{r^2}{h} + \frac{1}{2}gh^2 \end{bmatrix};\ \boldsymbol{S} = \begin{bmatrix} 0 \\ gh\left(S_{0,x} - S_{f,x}\right) \\ gh\left(S_{0,y} - S_{f,y}\right) \end{bmatrix};\ \boldsymbol{B} = \begin{bmatrix} q_b \\ \alpha_x q_b \\ \alpha_y q_b \end{bmatrix} \tag{2b}$$

where x and y stand for the space coordinates, h is the water depth, g represents the gravitational acceleration, q (resp. r) is the unit-discharge component in the x (resp. y) direction. $S_{0,X} = \partial z_b / \partial X$ (resp. $S_{f,X}$) is the bottom (resp. energy line) slope in the X-direction ($X = \{x, y\}$); z_b is the bottom elevation (also denoted as $z_{b,street}$ to avoid confusion with the building bottom elevation). $S_{f,X}$ is classically estimated using the Strickler formulae:

$$S_{f,X} = \frac{u_X\sqrt{q^2+r^2}}{K_x^2 h^{7/3}} \tag{3}$$

where K_X and u_X are respectively the Strickler coefficient and the flow velocity in the X-direction.

In the shallow water equations, the additional source term **B** is developed to account for local mass (first line of (2b)) and momentum balance (second and third lines of (2b)) modification in the street due to street-building exchanges.
The unit-discharge q_B is defined as:

$$q_b = \frac{\sum Q_i}{S} \tag{4}$$

where S is the area of the volume of control. α_x and α_y account for the effect of the street-building exchanges on the momentum balance in the street:

$$\alpha_x = \frac{q}{h};\ \alpha_y = \frac{r}{h} \text{ if } q_b > 0 \tag{5a}$$

$$\alpha_x = \alpha_y = 0 \text{ if } q_b \leq 0 \tag{5b}$$

When $q_b > 0$, the momentum in the volume of water leaving the street is taken out accordingly. Conversely, when $q_b < 0$, immobile water (with thus no momentum) is added to the street. This leads to an unmodified momentum while reducing the flow velocity.

The opening discharge is estimated using a classical weir law based on the geometry and both hydrodynamics in the street and in the building (**Figure 1**) depending on the regime [5, 12]. z_{street} and $z_{building}$ define the upstream and the downstream sides of the weir: the upstream being the side for which the free surface elevation is the higher at the beginning of the timestep.

$$Q_i = C_d w_{opening}\sqrt{2g}h_1^{\frac{3}{2}} \text{ if } h_2 \leq \frac{2}{3}h_1 \tag{6a}$$

$$Q_i = \frac{3\sqrt{3}}{2}C_d w_{opening}\sqrt{2g}h_2(h_1 - h_2)^{\frac{1}{2}} \text{ if } h_2 > \frac{2}{3}h_1 \tag{6b}$$

where $h_1 = \max(h_{w,street}; h_{w,building})$ and $h_2 = \min(h_{w,street}; h_{w,building})$ are respectively the water depth above the weir crest on the upstream and downstream side and C_d is a discharge coefficient. The first (resp. second) line of (6) corresponds to the unsubmerged (resp. submerged) case. By convention, Q_i is positive when the street is filling up the building ($z_{street} > z_{building}$) and negative when the building is emptying ($z_{street} < z_{building}$).

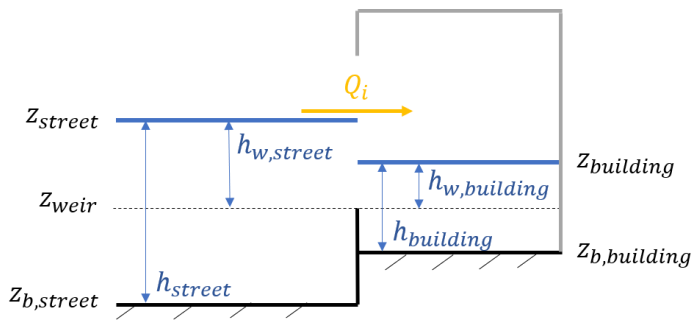

Figure 1: Schematic representation of the street-building exchanges in the transverse direction to the street axis. For the sake of clarity, the grey lines represent the building walls and roof but are currently not accounted in the street-building model.

The street-building exchanges model is implemented in the sw2d model[2]. Equations (1) and (2) are discretized using an explicit finite volume scheme. The source terms are solved using a classical time splitting method: the hyperbolic part of equation (2) and the bottom source terms are solved in a first time; the friction and building source terms are then calculated separately.

3. TEST CASES

[2] https://sw2d.inria.fr/

The ability of the proposed model to represent the flood dynamics in both the street and the buildings is assessed against two test cases. The first case presents a synthetic configuration to evaluate the potential effect of accounting the street-building exchanges. The comparison is then performed on a real-like test case based on the 1988 flood in Nîmes (France). A validation against several analytical test cases has been realized in simple configurations but is not presented here for the sake of simplicity.

3.1 Idealized street-building exchanges test case

3.1.1 *Presentation of the synthetic test case*

The synthetic test case evaluates the effect of the street-building exchanges on the flood propagation in a simple $15\ m$ width channel. An imposed hydrograph is injected at the upstream end (**Figure 2**). The channel is $5000\ m$ long and the duration is long enough ($30000\ s$) to ensure that the flow reaches the end of the channel. The downstream boundary condition imposes a Froude number equal to 1. The channel (i.e. the street) is meshed using a 1D-like approach: the cell width is equal to the channel width and the longitudinal discretization is $dx = 5\ m$. Dry initial conditions and uniform Strickler coefficient are set ($\mathrm{K} = 40\ m^{1/3}.\mathrm{s}^{-1}$).

For the simulation with buildings, 200 identical idealized buildings are equally distributed along the channel (1 building every $10\ m$ i.e. 1 building every 2 cells). Each building has a $100\ m^2$ area. The first building is linked to the first cell (from $x = 0$ to $5\ m$) and the last one is connected to the cell number 399th located between $x = 1990$ to $1995\ m$. For the sake of simplicity, the same opening is used to connect each building to the corresponding cell. Classical dimensions for a door are used for the width $w_{opening} = 0.9\ m$. The bottom elevation is identical in the building and in the street ($z_{b,street} = z_{b,building}$) and no step separate the building from the street ($z_{weir} = z_{b,street}$). An arbitrary but classical discharge coefficient $C_d = 0.42$ is used.

3.1.2 *Buildings effect in the street*

Figure 2a compares, at different locations, the discharge and the water level evolution in time with and without buildings. For both simulations, the maximal simulated variable (either street discharge or water depth) decreases along the street direction due to the natural flood spreading. For every location, accounting for the street-building exchanges lead to a reduction of both the maximal discharge and water level compared to the reference simulation without buildings. At $x = 2000\ m$ (corresponding to the end of the buildings area), the reduction reaches 30% of the discharge and 18% for the water depth. Furthermore, the peaks of discharge and water depth are delayed for the simulation with buildings; the delay increases with the distance. At $x = 2000$ m, the peak appears around $1000\ s$ later for the discharge and $2500\ s$ later for the water depth. Accounting for the buildings effect in a flood propagation model thus leads to a significant modification of the street hydrodynamics. Interestingly, after $16000\ s$ (end of the discharge injection at the inlet) the water levels and discharge curves converge and decrease slowly together, which can be related to the time for which the upstream discharge becomes nil.

Figure 2b presents the water depth along the street. The black and purple dotted lines correspond to the maximal water depth over the whole simulation with and without buildings. The water depths gap between the two simulations increases from the inlet to $x = 2000\ m$ (corresponding to the end of the buildings area) and then decreases while going downstream. This highlights the cumulative effect of the buildings on the flood propagation. **Figure 2b** also shows the flowlines for the configuration with building at different times. For $t > 16000\ s$ (end of the discharge injection at the inlet), the water levels are barely homogeneous for $x < 2000\ m$. Indeed, the difference between the maximal and minimal water depths represents 8 cm for $t = 16000\ s$ and is reduced around 4 cm for $t = 19000\ s$. In the meantime, the velocity does not exceed 0.2 m/s. This phenomenon is due to the nil discharge at the upstream end that acts an impervious boundary for $t > 16000\ s$. Moreover, at $19000\ s$, the flow reaches the downstream end of the channel and thus the flow is influenced by the downstream boundary condition. The following analysis concerning the buildings are thus carried out for $t < 16000\ s$, ensuring that the analysis is not influenced by the downstream boundary condition.

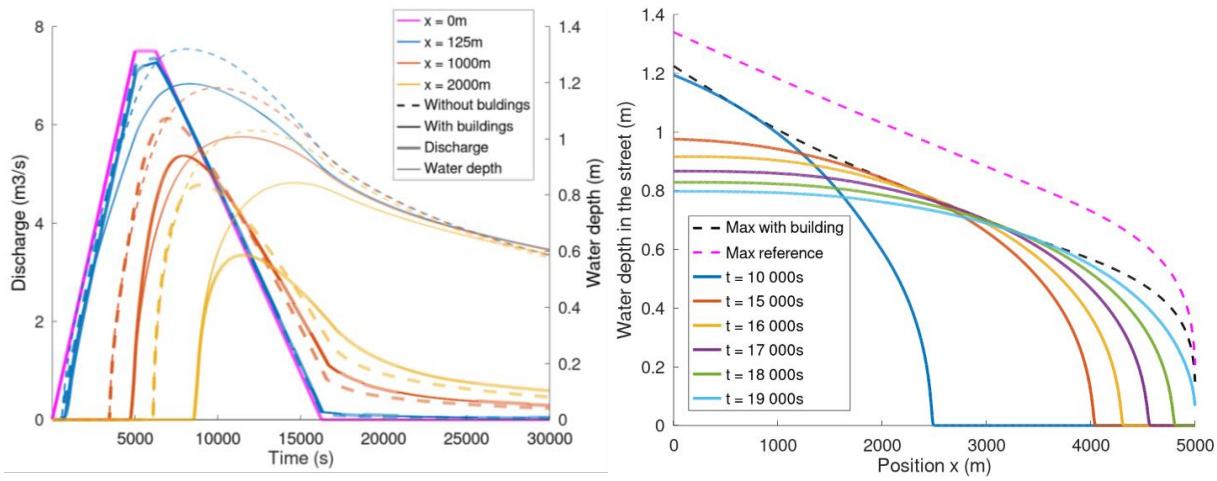

a **b**

Figure 2: Comparison of the street hydrodynamics with and without buildings. **a**: Discharge and water depth at different locations; **b**: Water depth along the channel at different time t (reference: simulation without any building, max: maximum water depth).

3.1.3 *Buildings water depth*

Figure 3a compares for several building the water depth evolution for $t < 16000\,s$. The maximal water depth within the building reaches 1.2 m for the 1st building (close to the inlet) and is reduced to 0.8 m for the last building. This reduction of the maximal water depth along the street axis is similar in the building and in the street (**Figure 2b**). The position of the building thus plays a significant role on the maximal water level reached during a flood event. Interestingly, the last building (building 200, x = 1995 m) has the steepest slope during its filling, which suggests the fastest filling speed.

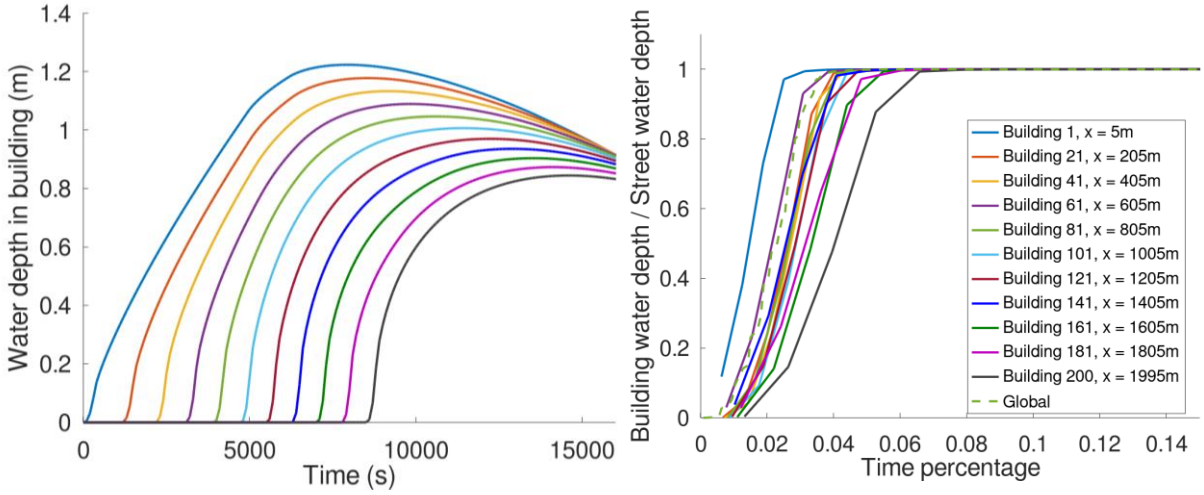

a **b**

Figure 3: Characterization of the hydrodynamics inside buildings (legend: building number and position). **a**: Water level evolution in time; **b**: Building and street water depth ratio.

Each building is linked to a single computational cell. Thus, it is possible to calculate the ratio $r(t)$ of the water depth in the building and the street for the buildings for each (stored) computational time:

$$r(t) = h_{building}(t)/h_{street}(t) \tag{7}$$

When $h_{street} = 0$ or $h_{buidling} = 0$, r is not computed. $\tilde{r}_i$ represents the ith value of $\tilde{r}$, the sorted chronicle of r. Since the storing time is constant, i/N (N the number of values in the chronicle) corresponds to the percentage of simulation time the ratio is smaller than $\tilde{r}_i$. **Figure 3b** presents $\tilde{r}$ for some single openings for $t < 16000\,s$. Considering the most left blue curve (building 1, $x = 5\,m$), $\tilde{r} = 0.8$ for $t = 0.02$; this indicates that the difference $h_{street} - h_{building}$ is bigger than $(1 - 0.8) * h_{street} = 0.2 * h_{street}$ only 2% of the plotted time (here $16000\,s$). This difference appears to be

significant only 7% of the time which indicates that the street and buildings have mostly the same water depth: $h_{building} = h_{street}$ 93% of the time. The difference is significative only during the beginning of the simulation that corresponds to the filling of the buildings. This very low dephasing between the street and the building water depth highlights the high conveyance of the openings; smaller conveyance should lead to more significative differences between the street and the building. The *global* curve on **Figure 3b** represents $\tilde{r}$ based on the values of $r(t)$ for all the openings together. The spreading around the *global* curve indicates the variety of the building hydrodynamics around the district average hydrodynamics.

3.2 Real configuration: Richelieu district in Nîmes, France

3.2.1 *Richelieu description*

The city of Nîmes (France) has suffered from a significant flooding on the 3rd of October 1988 with a return-period estimated between 150 and 250 years [6]. The Richelieu district was particularly impacted with water depths of up to 3 m in the streets. The present study aims to assess the interest of the proposed street-building model; the comparison will focus on the street hydrodynamics and the characterization of the building flooding.

For the sake of simplicity and to reduce the simulation time, the computational domain is limited to a subpart of the Richelieu district limited by the streets Faïta, Sully and Semard (**Figure 4a**). In this zone, the streets network is rather simple with intersections with an angle of barely 90°. The average slope is oriented from North to South and reaches 1%. The simulation domain is included in the whole Nîmes modeling constructed by INRAE[3] [16] that is thus used to provide the boundary conditions.

3.2.2 *Modeling of the street networks*

The streets network is extracted from the BD TOPO® (2020-12-15) and the 5 m DEM of the Gard department from the RGE ALTI® (2020-02-13) both from the French National Geographical Institute. The mesh is built such as having one to three cells of the street width (**Figure 4**).

The hydraulics conditions modeled by INRAE at the limits of the considered domain are set as boundary conditions. Upstream, the discharge is injected either at the upstream end of streets Sully and Vincent Faïta or at the connection between the Vincent Faïta street and those coming from the North. At the peak of the flood, the total injected discharge is 176 $m^3.s^{-1}$ with up to 92 $m^3.s^{-1}$ in the Sully street and 47 $m^3.s^{-1}$ in the Faïta street. At the downstream end, the free surface elevations computed by the INRAE modeling are imposed at the limits corresponding to an outlet street. They vary in the range of [0.46 m 1.77 m]. The simulation lasts 55000 s. For the friction, as in the INRAE model, a uniform Strickler coefficient $K = 40\ \mathrm{m}^{1/3}.\mathrm{s}^{-1}$ is applied [13].

3.2.3 *Building data*

The building limits are defined from the BD TOPO® thus allowing to compute their area $S_{building}$. For the sake of simplicity and due to the lack of data regarding the connections between buildings, only the ones directly along the street network are considered. Each building bottom elevation $z_{b,building}$ is computed as the mean elevation of the 5 m DEM from the RGE ALTI® within the building limits plus 0.19 m to account for the door elevation (see next paragraph). With this approximation, 50% of the buildings are 0.19 m above the street bottom elevation. Over the range of the modeled buildings, the bottom elevation $z_{b,building} - z_{b,street}$ lies in the range $[-42\ cm; 64\ cm]$. This suggests that for some buildings, the different rooms should have been modeled for a better representation of the storage capacity.

The INRAE field survey on doors and windows of the Catinat Street is used to characterize the modeled building openings. Based on 58 buildings (including 46 buildings in the simulated domain), the average dimensions have been determined (**Table 1**). The variability of the openings' height, width and elevation above the street ground is quite important. For the sake of simplicity, the same opening

[3] 'Institut national de recherche pour l'agriculture, l'alimentation et l'environnement

elevation is considered corresponding to the average field height and elevation above the street ground $(z_{weir} - z_{b,street})$.

Due to the lack of information on the precise location of the real openings, the assumption is used that each building wall (adjacent to the street) includes one single door and one single window. Each opening has the same weir height corresponding to the average dimension determined from the field survey. To account for the wall lengths variability, each opening width w' is computed as:

$$w' = L_{wall} \times n_{opening} \times w_{opening} \tag{8}$$

where L_{wall} is the length of the wall of the building adjacent to the street; $n_{opening}$ and $w_{opening}$ are the mean number of openings per building façade length and the mean opening width that has been estimated thanks to the field survey as defined in **Table 1**.

	width (m) $w_{opening}$	weir height (m) $z_{weir} - z_{b,street}$	Number of openings per unit length (m^{-1}) $n_{opening}$
Window	$1.10 + -0.38$	$1.12 + -0.27$	$0.12 + -0.10$
Door	$1.05 + -0.26$	$0.19 + -0.13$	$0.07 + -0.08$

Table 1: Mean dimensions (+- standard deviation) for openings from the field survey (Nîmes, France)

3.2.4 *Effects of buildings on the streets water depth*

Simulations without and with buildings are run; variables with subscript $h_{building}$ (resp. h_{ref}) correspond to the simulation with (resp. without) buildings. **Figure 4a** compares the maximal water depths in the two simulations: $\max(h_{building}) - \max(h_{ref})$. The difference of the maximal computed water depths is in the range $[-0.4\,m; 0.6\,m]$ highlighting that the street-building exchanges can be important to characterize the flood risk within the streets. The buildings lead to a reduction (right cells on **Figure 4a)** of the maximal water depth in the upstream (V. Faïta and Sully) streets and an increase (blue cells on **Figure 4a**) in the North-South streets and around the crossroad between the streets Richelieu and Catinat. This might suggest that the buildings modify the discharge partition between the inside of the district and the surrounding streets.

Figure 4b compares the maximum difference of the water depth at each time: $\max(h_{building} - h_{ref})$. Over the flood duration, the difference between the simulated water depth is in the range $[-0.6\,m; 0.8\,m]$ which is bigger than the difference on the maximal water depth. This indicates that the maximal differences are not reached at the flood peak but rather during the rising or the falling limb. The distribution of the differences between the maximal value and the maximal difference along the simulation are globally coherent even if some inversions can be identified (see for instance the western part of the Richelieu street). Moreover, during the simulation, some significant differences occur while the maximal value are identical in both simulations (see for instance the P. Semard street).

Similar analysis on the norm of the velocity vector (not presented here for the sake of concision) highlight that the modelled velocity differs up to $1.3\,m/s$; either positively or negatively. The comparison of both simulations highlights that the hydrodynamics can be significantly modified while accounting for the street-building exchanges.

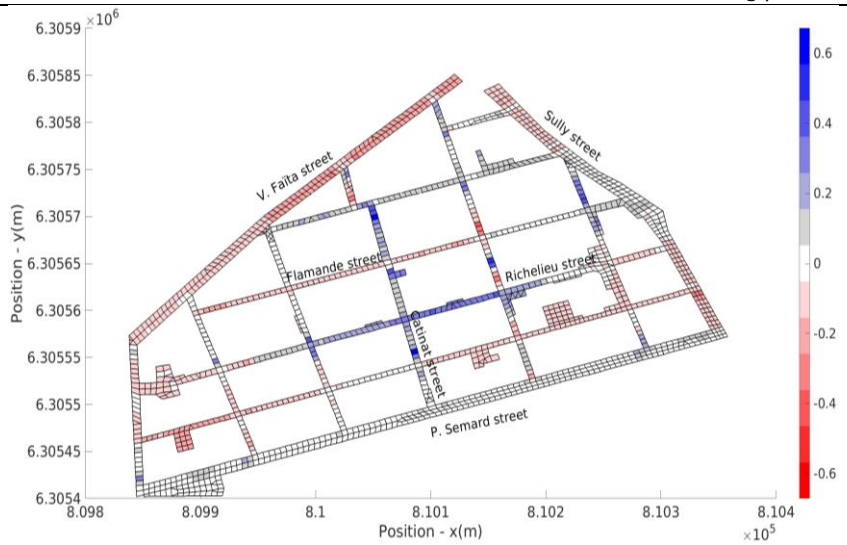

a

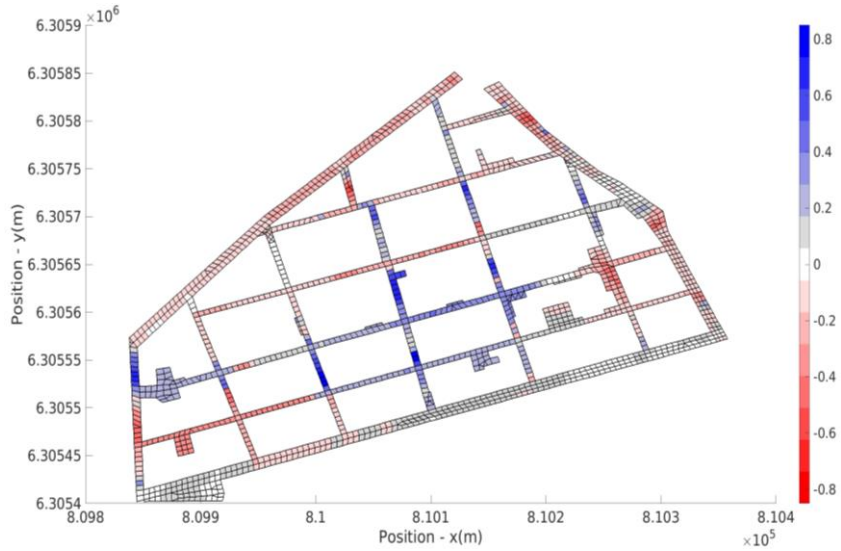

b

Figure 4: Comparison of the water depth computed in the streets with and without buildings. **a**: Difference of the maximal water depth ($\max(h_{building}) - \max(h_{ref})$); **b**: Maximal difference ($\max(h_{building} - h_{ref})$).

3.2.5 *Maximal water depth distribution*

The maximal water depths simulated in the buildings and in the streets are presented in **Figure 5**. The maximal water depth is up to 3.5 m which is coherent with what is known from the 1988 event. The North area is the most impacted. 9 over 438 simulated buildings are not flooded over the whole event (water depth = 0 m). The maximal water depth pattern in the buildings is globally coherent with the street distribution. However, significant differences can be highlighted for some buildings which might be explained by the gap between the bottom elevation of the building and the corresponding street (see section 3.2.3). The classical approach assuming the maximal water level in the building corresponds to the maximal free surface elevation [7] appears here to be valid.

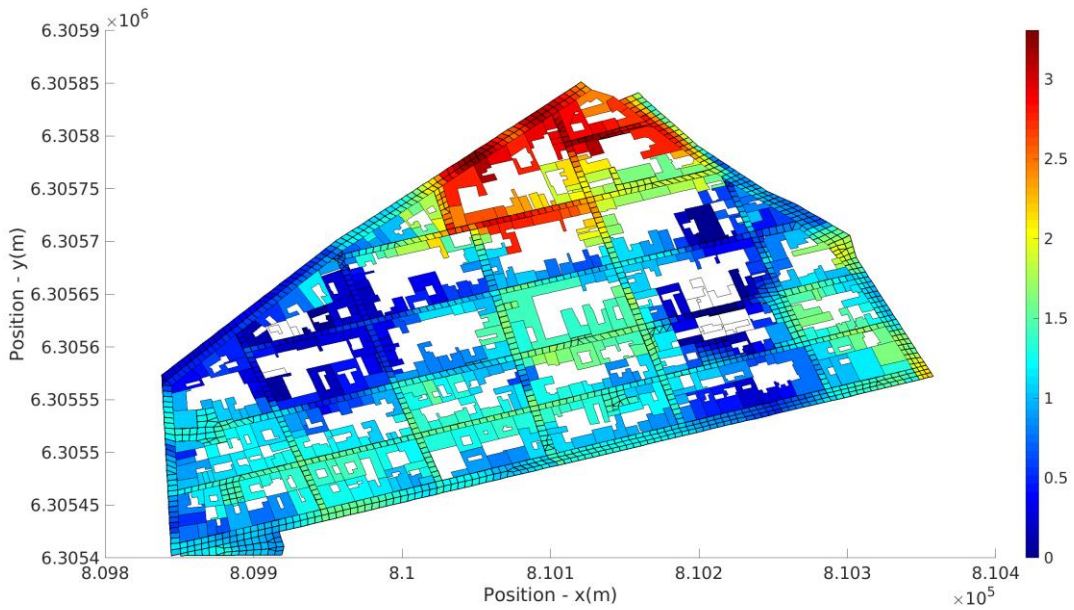

Figure 5: Maximal water depth in the streets and in the buildings.

3.2.6 *Buildings water depths evolution*

Each opening is associated to a surface elevation in the street and in the building. $\mathrm{d(t)}$ represents the surface elevation difference between both:

$$d(t) = z_{street}(t) - z_{building}(t) \tag{9}$$

Figure 6a shows the surface elevation difference for two openings in red and blue that reach the extremum values: the blue line achieves the maximum difference during the simulation and the red one the minimum. For the red line, 50% of the time the surface elevation in the building is greater than $0.5\ m$ above the one in the street. The blue line shows that the surface elevations are equals 15% of the time and for the rest, the surface elevation in the street is higher than the one in the building. These variable tendencies are possible because a building can have several openings connected to different mesh of the street, each mesh having its own bottom elevations. Thus, the results depend on the opening through which the surface elevations are observed (a building can be filled more quickly than it is drained and conversely) and on the bottom elevation difference of the building and the associated mesh. The bold black curve represents *d* for all the 1302 openings together. 60% of the time, the difference is nil, which means that the surface elevation of the building and the street are equals. The rest of the time is equally divided between the two possible cases: either the surface elevation in the street is above the one in the building and conversely. The maximum value is up to $1.16\ m$ and the minimum reaches -$0.76\ m$.

Figure 6b presents the cumulative curve of the submersion duration over the modelled buildings. A building is considered as flooded when the simulated water depth is positive. Interestingly, only a few buildings (26 over the 438 simulated buildings) are flooded for less than $6\ h$ and 50% of the buildings are flooded for more than $10\ h$. The spatial distribution of the duration should be characterized and related to the street geometry and building parameters and especially the location within the district (i.e. the vicinity to the inlet) and the number and conveyance of the openings. Moreover, except for the gap from 10 to $12\ h$, the trend appears to be quite similar. Further study should be investigated and try to confirm this particular feature.

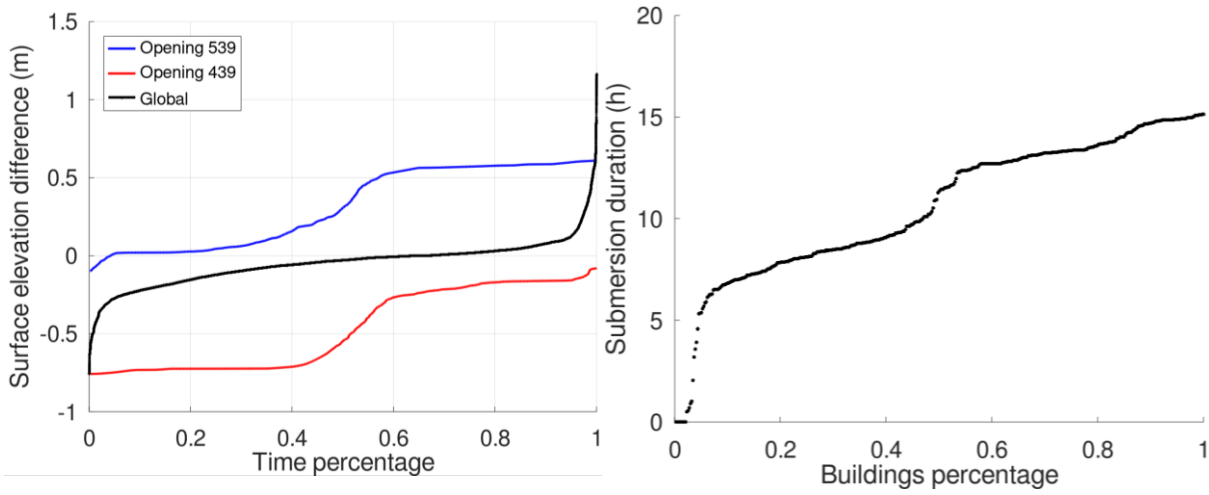

a **b**

Figure 6: Contributions of the model for economic perspectives. **a**: Building and street water surface elevation difference (m); **b**: Submersion duration (h).

4. CONCLUSION

Numerical models are frequently used to characterize and forecast flood impact especially in urban areas. In classical 2D approaches, the street-building exchanges remains neglected despite evidences from flood event feedbacks. The present paper proposes a new 2D modelling approach allowing to consider the exchanges between street and building during urban flood. Building water depth is modeled using a classical mass conservation law while opening discharge is represented with a weir law. This new model enables to compute both the street hydrodynamics using the 2D shallow water equations and the water depth evolution in buildings.

This model is validated against both an idealized urban test case and a real-world configuration representing the Richelieu district (Nîmes, France). Comparing the results with and without buildings allow to highlight their effect on the street flow. Accounting for the street-building exchanges lead to a significant modification of the street hydrodynamics. Over the range of the tested configurations, the street water is either increase or decrease of up to $60\ cm$. Subsequently, the flow velocity norm is modified of $1\ m/s$. Interestingly, the street depth modification is generalized in the idealized test case and more localized in the real-world simulation. These configuration-dependent effects pave the way to a wider study to be able to predict in which configuration the street-building exchanges play a significant role.

In the buildings, the modelling of the water depth evolution provides a new valuable information. Over the range of the tested configurations, several building patterns have been identified. In the idealized test case, the building water depth followed closely the street evolution highlighting the importance of the opening conveyance. In the Richelieu district simulation, the variability of the building flooding duration shows the interest of the proposed model to better characterize the flood impacts on the buildings and thus the potential damages. Moreover, the comparison of the free surface elevation in both the building and the linked street highlights significant differences (either positive or negative) occurring up to 60% of the flood duration. This information on the building dynamics might be of prime interest for flood damages and safety study.

The present work provides a relevant tool to better study the influence of the street-building exchange during an urban flood event. This preliminary work should be deepened by a sensitivity analysis on the discharge computation. Indeed, the present analysis is based on a simple weir law that might not be representative for some configurations highlighted in the real-world test case for which the free surface elevation reaches the top of the opening. The sensitivity analysis should also focus on the parameters of the opening laws. The Richelieu test case also pointed out the problematic of the representation of the buildings. The available data concerning the topography within the building

(bottom elevation, room organization and connectivity) is currently not available at a large scale. The sensitivity of the results to this information should also be investigated, either to state in which measure they can be roughly described or to identify a requirement of new types of data. Finally, an interdisciplinary study on flood damages and safety estimation can be based on the proposed model.

ACKNOWLEDGMENTS

This work has been supported by the French National Research Agency (ANR) under the grant ANR-18-CE01-0020.

REFERENCES AND CITATIONS

[1] Bazin, P.H., Nakagawa, H., Kawaike, K., Paquier, A., & Mignot, E. (2014). Modeling Flow Exchanges between a Street and an Underground Drainage Pipe during Urban Floods. Journal of Hydraulic Engineering, 140(10) :04014051.

[2] Beg, M.N.A., Carvalho, R.F., & Leandro, J. (2018). Effect of surcharge on gully-manhole flow. Journal of Hydro-environment Research,19, 224-236.

[3] Cea, L., Garrido, M., & Puertas, J. (2010). Experimental validation of two-dimensional depth-averaged models for forecasting rainfall–runoff from precipitation data in urban areas. Journal of Hydrology, 382(1): 88-102.

[4] CEPRI (2010). Guide Le bâtiment face à l'inondation.

[5] Cunge, J.A., Holly, F.M., & Verwey, A. (1980). Practical aspects of computational river hydraulics, Pitman, p169 and p266.

[6] Desbordes, M., Durepaire, P., Gilly, J.C., Masson, J.M., & Maurin, Y. (1989). 3 octobre 1988, Inondations sur Nîmes et sa région. Editions Lacour 1989.

[7] Eleuterio, J. (2012). Flood risk analysis: impact of uncertainty in hazard modelling and vulnerability assessments on damage estimations. PhD Thesis. Strasbourg University. Strasbourg, France.

[8] Finaud-Guyot, P., Garambois, P.A., Araud, Q., Lawniczak, F., François, P., Vazquez, J., & Mose, R. (2018). Experimental insight for flood flow repartition in urban areas. Urban Water Journal, 15(3): 242-250.

[9] Gems, B., Mazzorana, B., Hofer, T., Sturm, M., Gabl, R., & Aufleger, M. (2016). 3-D hydrodynamic modelling of flood impacts on a building and indoor flooding processes. Natural Hazards and Earth System Sciences, 16(6): 1351-1368.

[10] Ishigaki, T., Toda, K., & Inoue, K. (2003). Hydraulic model tests of inundation in urban area with underground space. In Proceedings 30th IAHR Congress, Thessaloniki, Greece, 487-493.

[11] LaRocque, L.A., Elkholy, M., Hanif Chaudhry, M., & Imran, J. (2013). Experiments on Urban Flooding Caused by a Levee Breach. Journal of Hydraulic Engineering, 139(9): 960-973.

[12] Mahmood, K., & Yevjevich, V. (1975). Unsteady Q (m3/s) in open channels, Volume 1 and 2. Water resources publications, Fort Collins, USA, p923.

[13] Mignot, E. (2005). Etude expérimentale et numérique de l'inondation d'une zone urbanisée : cas des écoulements dans les carrefours en croix. Thèse de doctorat. Ecole Centrale de Lyon. Lyon, France.

[14] Mignot, E., Camusson, L., & Riviere, N. (2020). Measuring the flow intrusion towards building areas during urban floods: Impact of the obstacles located in the streets and on the façade. Journal of Hydrology 583, 124607.

[15] Mignot, E., Zeng, C., Dominguez, G., Li, C.W., Rivière, N., & Bazin, P.H. (2013). Impact of topographic obstacles on the discharge distribution in open-channel bifurcations. Journal of Hydrology, 494, 10-19.

[16] Paquier, A., Tanguy, J.M., Haider, S., & Zhang, B. (2002) Estimation des niveaux d'inondation pour une crue éclair en milieu urbain : comparaison de deux modèles hydrodynamiques sur la crue de Nîmes d'octobre 1988. Revue des sciences de l'eau Rev. Sci. Eau 16, 2003, 911-934.

[17] Park, H., Cox, D.T, Lynett, P.J., Wiebe, D.M., & Shin, S. (2013). Tsunami inundation modeling in constructed environments: A physical and numerical comparison of free-surface elevation, velocity, and momentum flux. Coastal Engineering, 79: 9-21.

[18] Schubert, J.E., & Sanders, B.F. (2012). Building treatments for urban flood inundation models and implications for predictive skill and modeling efficiency. Advances in Water Resources, 41: 49-64.

[19] Smith, G.P., Rahman, P.F., & Wasko, C. (2016). A comprehensive urban flood-plain dataset for model benchmarking. International Journal of River Ba-sin Management, 14(3) :345-356.

[20] Sturm, M., Gems, B., Keller, F., Mazzorana, B., Fuchs, S., Papathoma-Köhle, M., & Aufleger, M. (2008). Experimental measurements of flood-induced impact forces on exposed elements. 40(9): 05005.

[21] Syme, W.J. (2008). Flooding in Urban Areas - 2d Modelling Approaches for Buildings and Fences. 9th National Conference on Hydraulics in Water Engineering: Hydraulics 2008, p25.

[22] Testa, G., Zuccala, D., Alcrudo, F., Mulet, J., & Soares-Frazao, S. (2007). Flashflood flow experiment in a simplified urban district. Journal of Hydraulic Research, 45 - Extra issue: 37-44.

[23] United Nations, Department of Economic and Social Affairs, Population Division (2019). World Urbanization Prospects: The 2018 Revision (ST/ESA/SER.A/420). New York: United Nations.

[24] Zhou, Q., Yu, W., Chen, A.S., Jiang, C., & Fu, G. (2016). Experimental Assessment of Building Blockage Effects in a Simplified Urban District. Procedia Engineering, 154: 844-852.